NeuroImage 277 (2023) 120242

Contents lists available at ScienceDirect

NeuroImage

journal homepage: www.elsevier.com/locate/neuroimage

State-dependent effectiveness of cathodal transcranial direct current stimulation on cortical excitability

Alessandra Vergallito[a,b,1,*], Erica Varoli[c,1], Alberto Pisoni[a,b], Giulia Mattavelli[d,e], Lilia Del Mauro[a], Sarah Feroldi[c], Giuseppe Vallar[a,b,f], Leonor J. Romero Lauro[a,b]

[a] Department of Psychology, University of Milano-Bicocca, Milano, Italy
[b] NeuroMi, Milan Center for Neuroscience, Milano, Italy
[c] School of Medicine and Surgery, University of Milano-Bicocca, Monza, Italy
[d] IUSS Cognitive Neuroscience (ICON) Center, Scuola Universitaria Superiore IUSS, Pavia, Italy
[e] Istituti Clinici Scientifici Maugeri IRCCS, Cognitive Neuroscience Laboratory of Pavia Institute, 27100, Italy
[f] MiBTec - Mind and Behavior Technological Center, University of Milano-Bicocca, Milan, Italy

ARTICLE INFO

Keywords:
tDCS
Cathodal tDCS
TMS-EEG
State-dependency

ABSTRACT

The extensive use of transcranial direct current stimulation (tDCS) in experimental and clinical settings does not correspond to an in-depth understanding of its underlying neurophysiological mechanisms. In previous studies, we employed an integrated system of Transcranial Magnetic Stimulation and Electroencephalography (TMS-EEG) to track the effect of tDCS on cortical excitability. At rest, anodal tDCS (a-tDCS) over the right Posterior Parietal Cortex (rPPC) elicits a widespread increase in cortical excitability. In contrast, cathodal tDCS (c-tDCS) fails to modulate cortical excitability, being indistinguishable from sham stimulation.

Here we investigated whether an endogenous task-induced activation during stimulation might change this pattern, improving c-tDCS effectiveness in modulating cortical excitability.

In Experiment 1, we tested whether performance in a Visuospatial Working Memory Task (VWMT) and a modified Posner Cueing Task (mPCT), involving rPPC, could be modulated by c-tDCS. Thirty-eight participants were involved in a two-session experiment receiving either c-tDCS or sham during tasks execution. In Experiment 2, we recruited sixteen novel participants who performed the same paradigm but underwent TMS-EEG recordings pre- and 10 min post- sham stimulation and c-tDCS.

Behavioral results showed that c-tDCS significantly modulated mPCT performance compared to sham. At a neurophysiological level, c-tDCS significantly reduced cortical excitability in a frontoparietal network likely involved in task execution. Taken together, our results provide evidence of the state dependence of c-tDCS in modulating cortical excitability effectively. The conceptual and applicative implications are discussed.

1. Introduction

Over the past decades, transcranial direct current stimulation (tDCS) has emerged as a non-invasive, cheap, safe, and easy-to-use technique to modulate cortical excitability in healthy volunteers and patients (Berryhill and Martin, 2018; Fregni et al., 2020). Despite its massive use, knowledge of tDCS physiological mechanisms remains incomplete.

Unlike Transcranial Magnetic Stimulation (TMS), which can induce post-synaptic excitatory potentials, tDCS is a neuromodulatory technique. Indeed, the current reaching the cortical surface is too weak to generate action potentials per se. Still, it is enough to alter the excitability and the spontaneous neural firing rate during and after the end of stimulation (Bocci et al., 2020; Nitsche et al., 2008; Stagg et al., 2018). It is common knowledge that the modulatory effects of tDCS depend on the polarity of stimulation, with anodal tDCS (a-tDCS) increasing firing rate, hence excitability, and cathodal (c-tDCS) leading to the opposite outcome (Bindman et al., 1964; Creutzfeldt et al., 1962; Nitsche and Paulus, 2000; Purpura and McMurtry, 1965). This physiological evidence has wrongly been extended to behavioral and psychophysiological measures, oversimplifying the cerebral dynamics underlying complex responses (Bradley et al., 2022). Evidence is indeed controversial concerning the established anodal-excitatory and cathodal-inhibitory coupling (Jacobson et al., 2012; Schroeder and Plewnia, 2017), and non-linear effects have been reported for both stimulation polarities (Batsikadze et al., 2013; Hassanzahraee et al., 2020; Mosayebi-Samani et al., 2023; Samani et al., 2019). Evidence from stud-

* Corresponding author at: Department of Psychology, University of Milano-Bicocca, Piazza Ateneo Nuovo, 1, 20126 Milano, Italy.
E-mail address: alessandra.vergallito@unimib.it (A. Vergallito).
[1] AV and EV contributed equally to this work

https://doi.org/10.1016/j.neuroimage.2023.120242.
Received 6 March 2023; Received in revised form 9 June 2023; Accepted 20 June 2023

ies investigating mechanisms underneath the complex pattern of reported findings is still unclear. Much literature has neglected this issue, opting to use only a-tDCS to explore the brain-cognition interface or to treat different pathological conditions (Dedoncker et al., 2016) since it results more effective in modulating behavior (Jacobson et al., 2012).

Among the advantages of using tDCS compared to TMS, there is the possibility of synchronously combining brain stimulation with a concurrent behavioral or cognitive task/training with minor exogenous distractions and somatosensory sensations. This option seems particularly convenient, considering that several studies highlighted that non-invasive brain stimulation (NiBS) effects are *state-dependent;* namely, they are influenced by the current ongoing activity of the stimulated regions (Bikson and Rahman, 2013; Pisoni et al., 2018; Siebner et al., 2009). Evidence from in vivo and in vitro studies indicates that a synaptic activity simultaneous with the stimulation is needed to induce detectable effects of tDCS (Cambiaghi et al., 2010; Priori et al., 1998). State-dependency mechanisms are largely unknown, although they could have crucial implications for basic research and clinical translation. According to the network activity-dependent hypothesis, tDCS effects would modulate neurons already engaged in an ongoing activity because they are close to the discharge threshold (Siebner et al., 2009). Therefore, stimulation delivered concurrently with a task recruiting the same neural network may induce a synergistic relationship between the endogenous neural activity generated by task execution and the exogenous source of activity promoted by the tDCS (Martin et al., 2014; Ohn et al., 2008; Stagg and Nitsche, 2011). Similarly, Bikson & Rahman (Bikson and Rahman, 2013) suggest that a functional property of tDCS is "activity-selectivity", referring to the preferential modulation of the activated rather than inactive neuronal networks. Such property would also explain how tDCS can induce task-specific changes in brain activity despite being considered a technique with a low spatial focality. Critically, neurophysiological evidence in this sense has been provided in both the animal model and humans (Fritsch et al., 2010; Pisoni et al., 2018).

The concept of state dependency might represent a step forward in understanding many aspects of tDCS use. For instance, the influence of brain state in modulating tDCS effects can help explain polarity asymmetries and the variability of tDCS effects (Li et at., 2015b; Ridding and Ziemann, 2010; Vergallito et al., 2022). Studies are indeed typically heterogeneous considering the coupling of brain stimulation and cognitive tasks, sometimes delivering tDCS before the task (as priming), sometimes during (as synergistic), and more rarely after (as consolidator) (Tatti et al., 2022). State dependency might also play a role in the reported lack of effectiveness of c-tDCS. Indeed, applying c-tDCS at rest (as in offline protocols) may fail to induce modulation in brain activity and behavior since a certain background activity might be needed to detect such an effect (Bortoletto et al., 2015; Matsunaga et al., 2004). Related to state dependency, in a recent study combining tDCS with functional magnetic resonance imaging (fMRI), Li and colleagues (Li et al., 2019) designed a factorial experiment manipulating the cognitive state (Choice Reaction Task vs. rest condition) and the stimulation polarity (anodal, cathodal, and sham). They delivered a short stimulation protocol over the right inferior frontal gyrus. When applied at rest, a-tDCS had a more pronounced effect compared to c-tDCS, increasing activation within the default mode network (DMN), which is typically active when individuals are not engaging in a specific activity or task, and decreasing activation of the salience network (SN), which responds the subjective salience of stimuli (internal or external). C-tDCS effects were greater during task execution, where both stimulations increased SN activity.

The state-dependent effect of tDCS, as highlighted by Li et al. (2019), partially aligns with the results from previous studies of our research group. Indeed, we assessed the effects on brain excitability induced by tDCS using a system combining TMS with electroencephalography (TMS-EEG). Specifically, at resting state, a-tDCS over the right posterior parietal cortex (rPPC) elicited a widespread excitability increase along a bilateral frontoparietal network, likely overlapping the DMN (Romero Lauro et al., 2014, 2016). Conversely, despite maintaining the same parameters (duration, intensity, electrode size, and montage), c-tDCS failed to modulate cortical excitability, being indistinguishable from sham stimulation (Varoli et al., 2018). These results thus confirmed the reported imbalance of a-tDCS vs. c-tDCS (Dedoncker et al., 2016; Jacobson et al., 2012) at the resting state. Notably, when a-tDCS was delivered over the left inferior frontal gyrus during a fluency task, the increase in excitability rather than widespread was selective for the brain regions involved in task performance (Pisoni et al., 2018). Moreover, a-tDCS improved behavioral performance, and such enhancement positively correlated with changes in excitability.

In the present study, we aimed to complement our previous results, in which c-tDCS was applied at rest (Varoli et al., 2018), with a new experiment in which tDCS was coupled with concurrent tasks involving the same stimulated brain network. To do so, we kept the stimulated region (rPPC) and the tDCS parameters of Varoli et al. (2018) unchanged. We used two visuospatial tasks: one tapping visual working memory (VWMT) (Heimrath et al., 2012; Vogel and Machizawa, 2004) and the other involving attention reorienting, namely a modified version of the Posner Cueing task (mPCT) (Arif et al., 2020; Spooner et al., 2020). Tasks were chosen because the rPPC seems to be a junction region between the cerebral circuits underlying visuospatial working memory and visuospatial orienting attention (Chica et al., 2013; Juan et al., 2017). During visual working memory tasks, brain activation has been shown to co-occur across the rPPC and the dorsolateral prefrontal cortex (Friedman and Goldman-Rakic, 1994). On the other side, neurophysiological, neuroimaging, and neuropsychological studies have consistently supported the critical role of rPPC in directing attention (Behrmann et al., 2004; Corbetta et al., 2000; Corbetta and Shulman, 2002; Thakral and Slotnick, 2009; Vallar and Perani, 1986).

We ran a first study in which sham and c-tDCS were delivered over the rPPC during the execution of the tasks to assess whether the stimulation could induce a behavioral effect on the participants' performance. Once we had established the feasibility of modulating mPCT performance through c-tDCS, we ran a second experiment, applying TMS-EEG in a new sample of participants to track the impact on cortical excitability of delivering c-tDCS during a cognitive task. The TMS-EEG procedure was identical to that of Varoli et al. (2018), where c-tDCS was delivered at rest. At variance from this previous research, here we expected to detect a neurophysiological effect of c-tDCS, possibly reducing excitability within the cortical network engaged in task execution.

2. Experiment 1

2.1. Materials and methods

2.1.1. Participants

Thirty-eight students (fourteen males, mean age = 22.8 years, SD = ± 4.1) participated in the study. Participants were right-handed according to the Edinburgh Handedness Inventory (Oldfield, 1971) (M = 0.88, SD = ± 0.13) and had no contraindications to NiBS (Antal et al., 2017; Rossi et al., 2021; Rossi et al., 2009). The experiment occurred in the Department of Psychology at the University of Milano-Bicocca. The Ethics Committee approved the study, and the participants' treatment followed the principles stated in the Declaration of Helsinki. The sample size (at least N = 36) was estimated through an a-priori power analysis using G-Power 3.1 (Faul et al., 2007). The power analysis was based on a within-factors repeated measures ANOVA with a small effect size = 0.20, α = 0.05, and power = 0.80.

2.1.2. TDCS stimulation

TDCS was delivered by a BrainSTIM standard stimulator (EMS, Bologna, Italy). To keep unchanged the tDCS parameters applied in our previous studies (Romero Lauro et al., 2014; Varoli et al., 2018), we set the current intensity at 0.75 mA and delivered it through the cathode (9 cm^2, density 0.08 A/m^2) placed over the rPPC (P2) and the anode (25 cm^2, density 0.03 A/m^2) over the left supraorbital area. Therefore, the

term c-tDCS refers to the polarity of the electrode placed over the rPPC. Stimulation was delivered for 15 min, with a 10 s fade-in/fade-out period. Parameters were in line with tDCS guidelines (Nitsche et al., 2008). In the sham condition, the procedure was kept identical to c-tDCS. Still, current was delivered only for the first 30 s, a procedure typically used to make participants blind to the assigned condition since the sham tDCS elicits similar skin sensations compared to real tDCS (Ambrus et al., 2012; Gandiga et al., 2006; Mattavelli et al., 2022; Woods et al., 2016).

2.1.3. Tasks

2.1.3.1. Modified Posner Cueing task. In the mPCT, the trials followed the subsequent structure: i) a fixation cross was positioned at the center of a black screen for 2000 ms; ii) two gray squares appeared on the left and right side of the fixation cross; iii) after an interval ranging from 200 to 700 ms, the outline of one of the two squares became red (cue) for 100 ms; iv) both squares remained gray for 100 ms; v) a small gray square (target) appeared inside the left or right squares and remained on the screen until participant response for a maximum time of 2000 ms (see Fig. 1– Panel A for a graphical representation). During the task, participants were instructed to focus on the fixation point and detect the target as accurately and fast as possible, pressing the letter "F" on the Italian keyboard for targets appearing in the left square and "J" for stimuli presented to the right.

Two combinations of cue and target locations were possible: a valid or congruent condition, in which the target appeared on the same side of the cue, and an invalid or incongruent condition, in which the target and the cue appeared on the opposite sides. The mPCT comprised 48 congruent (24 on the right side and 24 on the left side of the central cross) and 48 incongruent trials (24 on the right and 24 on the left side of the central cross). Ten false alarm trials were added, in which no targets followed the cues. False alarms were not analyzed since participants did not have to press any key. We collected data using E-Prime 2 Software (Psychology Software Tools, Pittsburgh, PA). Response accuracy and reaction times (RTs) were recorded.

Notably, in the mPCT we changed the proportion of valid and invalid trials compared to the classic version of PCT (cPCT): whereas in the cPCT, the typical ratio of valid and invalid trials is 80% and 20%, respectively (Posner, 1980; Posner et al., 2014), the mPCT comprised an equal amount of valid and invalid trials (Arif et al., 2020; Spooner et al., 2020). The rationale for increasing the number of invalid trials in the mPCT, compared to the cPCT, was that we were planning to use the task in the subsequent TMS-EEG study. For methodological reasons, we then needed a sufficient and comparable number of trials for valid and invalid conditions to achieve reliable TMS Evoked Potentials (TEPs). We validated the mPCT in a pilot experiment described in the Supplementary materials (Section A).

2.1.3.2. Visual working memory task. The VWMT consisted of two blocks of 48 trials each, separated by a 30 s time interval. In each trial, participants maintained their gaze fixed on a central cross. After 2000 ms, an arrow appeared on the top of the fixation point for 200 ms, and it could point either to the left or to the right hemifield, followed by a visual matrix comprising eight colored dots (size = 80 pixels; diameter = 1.75 cm), half localized on the right side and half on the left side of the screen. Within any visual matrix, all eight dots appeared with a different color and in a different position, varying within a rectangular portion of the hemifield. The colors and the positions were randomly assigned to avoid the compresence of two or more dots with the same shade and to reduce any facilitation effects. The visual matrix lasted 250 ms on the screen and was followed by a retention interval of 2000 ms. After that, a colored dot (target stimulus) appeared at the center of the screen and participants had 2000 ms to establish if the displayed target was included (80% of the trials) or not (20%) in the initial matrix taking into consideration its color and ignoring its position (see Fig. 1– Panel B for a graphical representation). Participants were asked to press two keys on the keyboard to perform their choices using their index fingers. Due to the great difficulty of the task, evaluated by preliminary pilot subjects, participants completed a training session of 48 trials.

2.1.4. Experimental procedure

Participants underwent two sessions, at least 48 h apart (Nitsche et al., 2008), which differed only in the type of stimulation (c-tDCS or sham) they received. In each session, they performed the mPCT and the VWMT in a counterbalanced order. Both tasks were performed using a laptop (15.7″ screen) at a distance of 60 cm from the participants. The order of stimulation conditions was counterbalanced across participants.

2.1.5. Statistical approach

MPCT and VWMT were analyzed separately. We performed analyses in the statistical programming environment R (R Core Team, 2022).

For the mPCT, we analyzed the dichotomous variable accuracy using general mixed effects models (Baayen et al., 2008), fitted using the GLMER function of the lme4 R package (Bates et al., 2015). RTs values were analyzed using linear mixed-effects regression using the LMER procedure in the same lme4 package. The *trial validity* (factorial, two levels: valid vs. invalid), *tDCS condition* (factorial, two levels: cathodal vs. sham), and their interaction were entered in the full model as fixed factors. Moreover, we added the simple effect of the *trial order* to account for changes in performance due to learning or fatigue effects. A by-subject random intercept was included to account for participant-specific variability (Baayen et al., 2008). Fixed predictors' inclusion in the final models has been tested with a series of likelihood ratio tests (LRT) by progressively removing parameters that did not significantly increase the overall model goodness of fit (Gelman and Hill, 2006). For RTs, the automatic procedure step was used, while for the accuracy variable, this procedure was performed manually. Only RTs from accurate responses were included in the analyses. Outliers were removed using model criticism, a data-driven procedure in which the full model was fitted and then the extreme standardized residual values were removed (2.5 SD) (Baayen and Milin, 2010; Baayen, 2008).

Concerning the VWMT, in line with previous studies (Heimrath et al., 2012), we calculated the WM capacity K factor (Cowan, 2001; Pashler, 1988). This index assesses the individual WM performance for each *tDCS condition* (cathodal vs. sham) and *attending hemifield* (left vs. right). K factor was estimated for each subject using the following formula: $K = S\ (H - F)$. In the procedure, K represents the number of items that can be held in WM from an array of S objects. It assumes that the target item would have been stored in memory with respect to K/S of trials such that the performance will be correct on K/S on the change trials (= hit rate H). This procedure also considers the false alarm rate F to correct for guessing. In our statistical procedure, the continuous index K was analyzed using linear mixed models. We included participants' intercept as a random structure, while *tDCS condition* (two levels: cathodal and sham) and *attended hemifield* (two levels: left vs. right) plus their interaction were added as fixed factors in the full model. As for the mPCT, we applied the automatic procedure step to remove the parameters that did not increase the model's goodness of fit.

For details on the model selection, see Supplementary Materials (Section B).

2.2. Results

2.2.1. mPCT

All false alarms and the data from two participants were excluded from analyses due to the low level of accuracy in one of the experimental sessions (one participant performed accurately in 52% of trials and the other 49%). Therefore, the analyzed sample included 36 participants. Statistical analysis for accuracy was run on 6912 data points.

The best-fitting model included the simple effect of *trial validity* and *trial order* ($\chi^2_{(1)} = 8.3$, $p = .004$). Considering the simple effect of *trial*

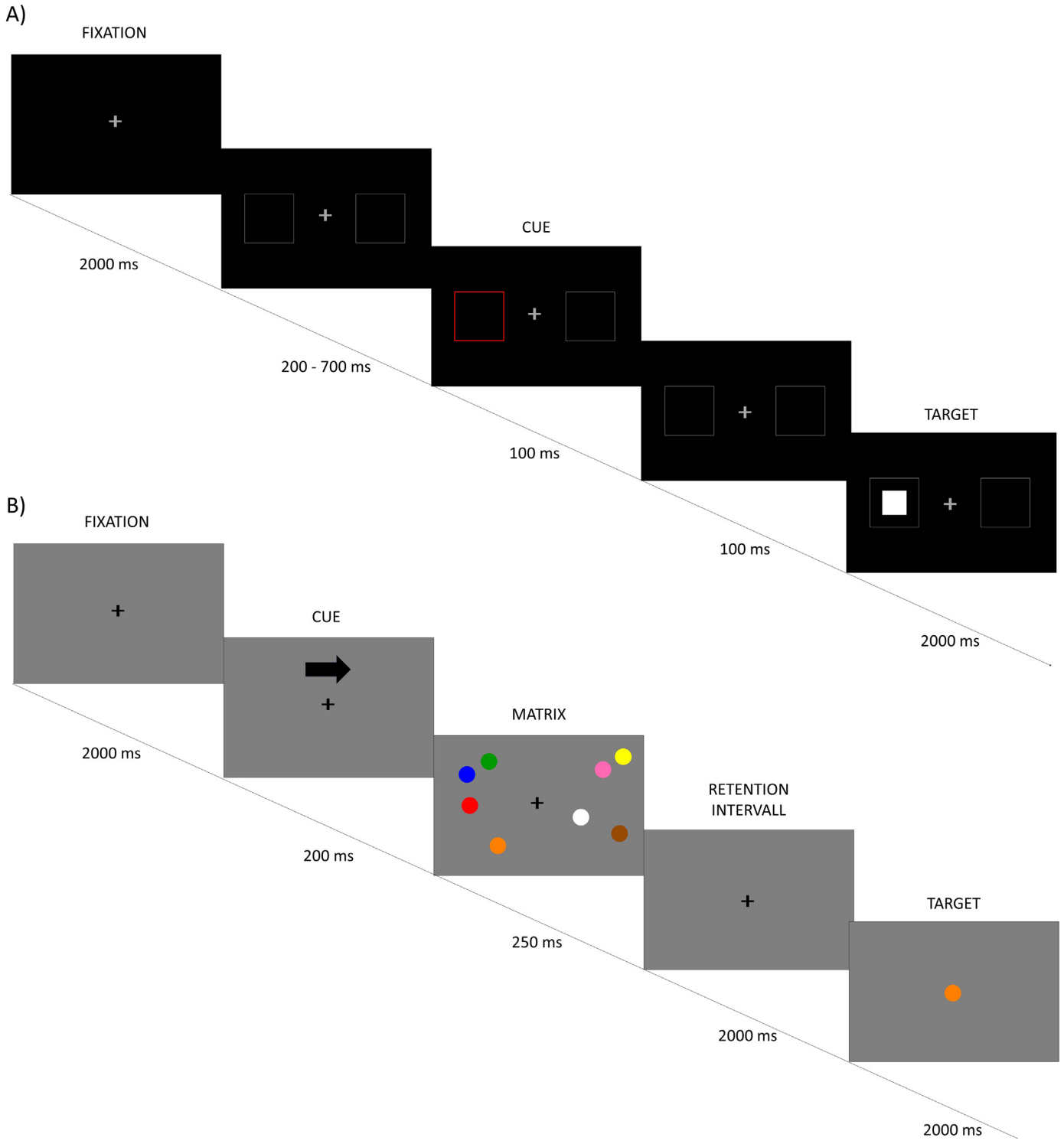

Fig. 1. Graphical representation of the tasks' procedure. Panel A highlights the mPCT procedure, with an example of a valid trial. Panel B represents a trial of the VWMT in which the target was included in the presented matrix.

validity, accuracy was higher in the valid ($M = 99.4$, SD $\pm$ 7.8) compared to the invalid ($M = 97.8$, SD $\pm$ 14.8) condition ($p < .001$). Concerning the effect of *trial order*, performance linearly increased during the experiment performance ($p = .004$).

Concerning RTs, we ran the analyses on 6814 data points. The best-fitting model included the simple effect of *trial order* and the interactions between the *tDCS condition* and *trial validity* ($\chi^2_{(1)} = 11.2$, $p = .001$). Considering the effect of *trial order*, RTs decreased during task performance, showing a learning effect ($\chi^2_{(1)} = 41.1$, $p < .001$). Relative to the interaction between *tDCS condition* and *trial validity* ($\chi^2_{(1)} = 11.2$, $p = .001$), post-hoc analysis showed that in the sham condition, a difference was traceable between valid and invalid presentations, with faster RTs in the valid condition ($p < .001$) while no differences were traceable for the cathodal stimulation ($p = .940$). Moreover, in the valid condition, RTs were slower in the cathodal stimulation compared to the sham condition ($p = .021$). Conversely, in the invalid condition, RTs were faster

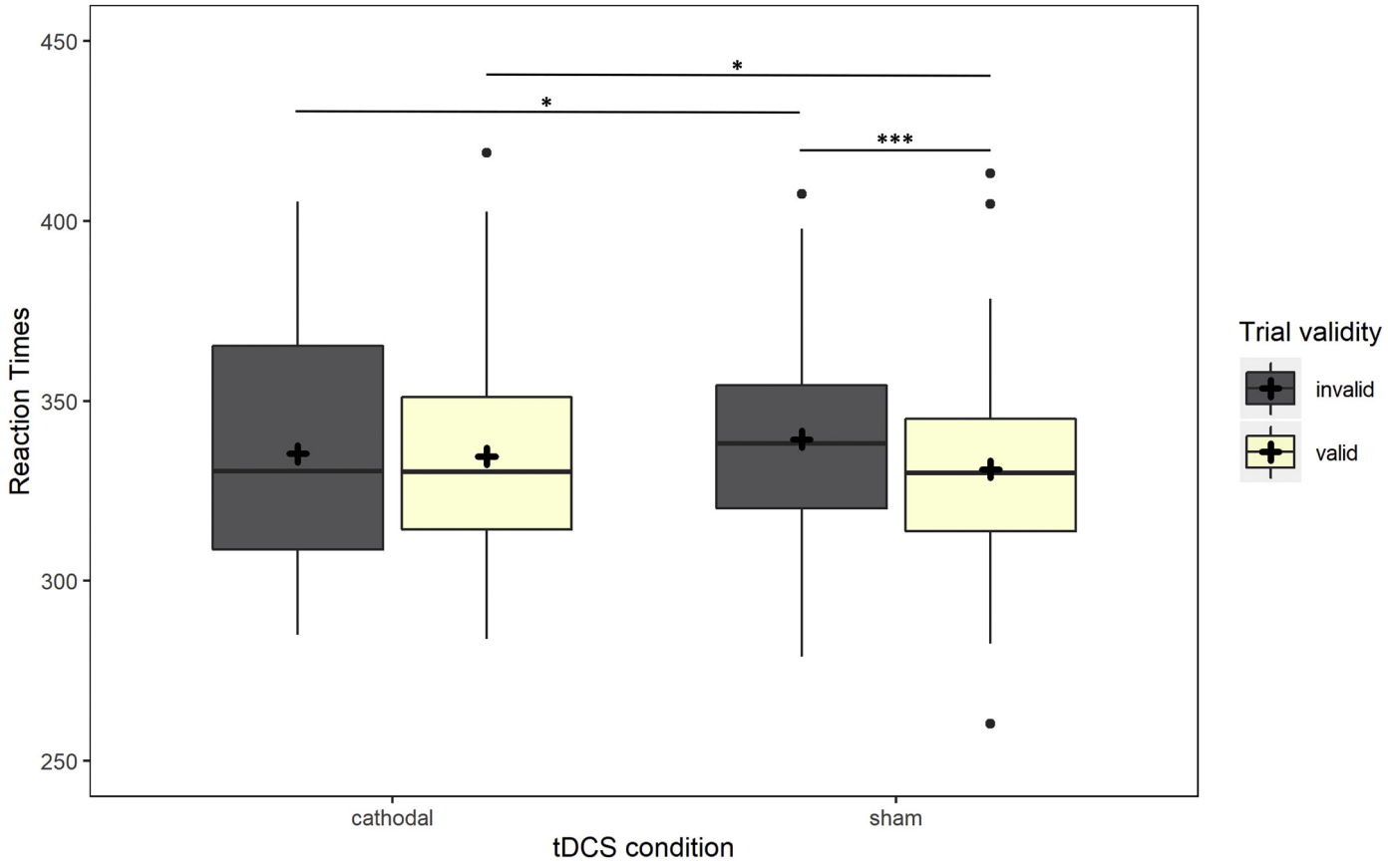

Fig. 2. Results on RTs data in Experiment 1. The boxplots represent the RTs comparison between valid (light yellow boxes) and invalid (dark gray boxes) trial conditions in the c- and sham tDCS sessions, on the left and the right, respectively. Asterisks represent statistical p-values *** $p < .001$. ** $p < .01$, * $p < .05$.

in the cathodal vs. sham condition ($p = .021$) (see Fig. 2 for a graphical representation).

2.2.2. VWMT

One participant was removed due to a technical problem during task execution. The analysis was run on 148 data points. The best model was the one without a fixed factor (See Table S5). Therefore, no significant differences were found between the two stimulation conditions, the attended hemifields, nor their interaction.

2.3. Interim conclusions

The results from Experiment 1 shed light on the feasibility of using c-tDCS over rPPC to modulate task performance in one of the two selected visuospatial tasks, namely mPCT. We observed indeed that c-tDCS abolished the advantage for valid cues. After having tested the behavioral effects of c-tDCS over the rPPC in modulating performance in a visuospatial task, we proceeded to Experiment 2 to explore the neurophysiological underpinnings of such modulation and to test our main hypothesis, i.e. whether neurophysiological effects on cortical excitability might arise when c-tDCS over rPPC is delivered during a task which involves this brain region.

3. Experiment 2: TMS-EEG

3.1. Materials and methods

3.1.1. Participants

Sixteen healthy volunteers (seven males, mean age = 25.4 years, SD = ± 3.5), different from those involved in Experiment 1, participated in Experiment 2. They were right-handed (mean laterality coefficient = 0.89, SD = ± 0.14) and were included following the same criteria as Experiment 1. We did not run an a priori power analysis to estimate the sample size, rather we based it on previous TMS-EEG studies with similar aims and procedures (Romero Lauro et al., 2014; Varoli et al., 2018; Hill et al., 2018; Grasso et al., 2021)

3.1.2. Procedure

All volunteers participated in two experimental sessions, performed at least one week apart, corresponding to c-tDCS and sham conditions. The order of the tDCS conditions was counterbalanced across participants. Each session consisted of two blocks of TMS-EEG recordings performed before (pre-tDCS) and 10 min after the end of tDCS stimulation (post-tDCS) (see Fig. 3 for a schematic representation of the procedure). Considering that c-tDCS affected performance only in the mPCT and that previous evidence suggested that tDCS has a cumulative effect on performance (Boggio et al., 2008; Monte-Silva et al., 2010), we decided to present the two tasks in a fixed order to maximize behavioral modulation. Therefore, in Experiment 2, participants performed first the VMWT (duration ~ 7 min) and then the mPCT (duration ~ 8 min). To allow the comparison with our previous study in which c-tDCS was delivered at resting state (Varoli et al., 2018), all the experimental parameters except tasks' execution were kept identical. In particular, the choice of stimulating 10 min after the end of stimulation was originally based on studies that observed that the effectiveness of c-tDCS (Antal et al., 2004) in modulating early components of visual evoked potentials starts 10 min after the end of stimulation.

3.1.3. TDCS parameters

We applied the same stimulation parameters used in Experiment 1. The cathode was placed under the P2 EEG electrode, previously removed from the cap (see Fig. 4– Panel b for the tDCS estimated electric field).

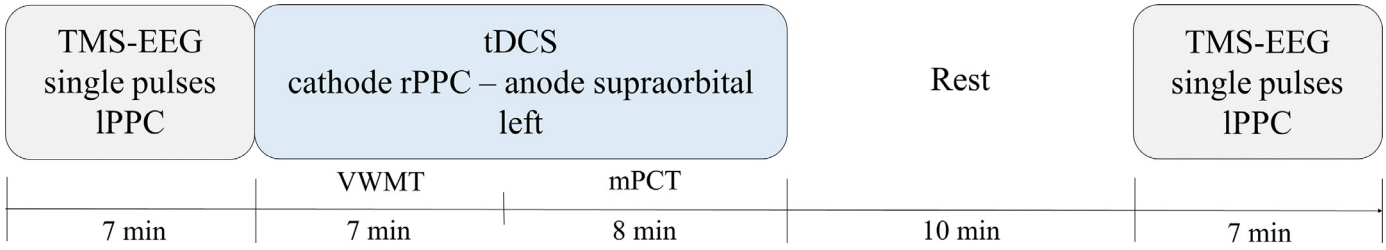

Fig. 3. A graphical pipeline of the TMS-EEG experimental procedure. The gray boxes represent the two TMS-EEG recordings before and (10 min) after cathodal and sham tDCS delivery. The cyan box represents the tDCS session, in which 0.75 mA tDCS was delivered with the cathode (3 × 3 cm) placed over the rPPC and the anode (5 × 5 cm) over the left supraorbital region. During tDCS, participants performed a VWMT (7 min) followed by the mPCT (8 min).

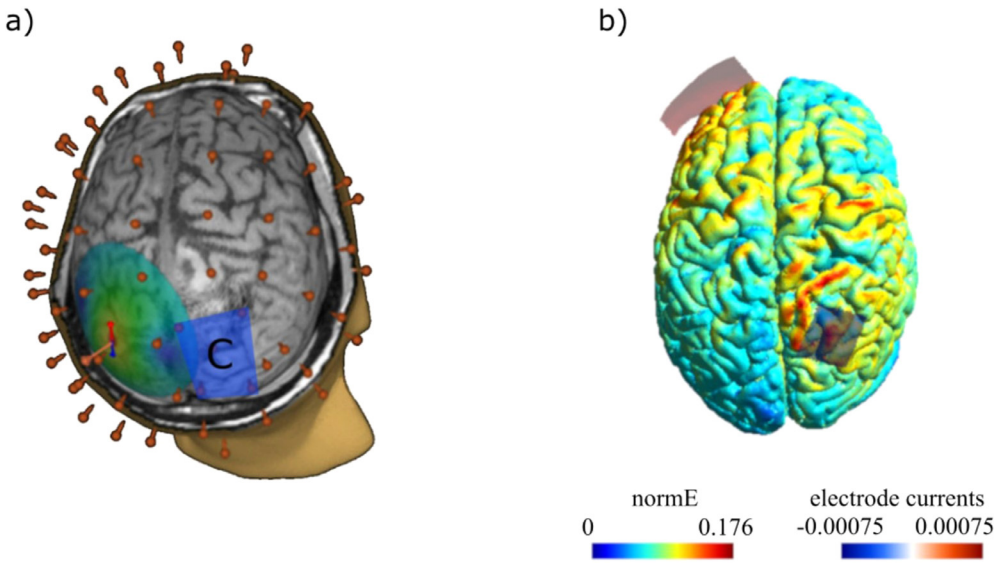

Fig. 4. TDCS and TMS-EEG setting. Panel a: individual MRI 3D reconstruction showing the TMS electrical field on the left PPC (where TMS single pulses were delivered). The blue rectangle represents the cathode position over the rPPC; the 60 red points correspond to the EEG electrodes. Panel b: the tDCS estimated current flow.

3.1.4. TMS-EEG parameters

For TMS-EEG recording, single pulses of TMS were delivered with an Eximia™ TMS stimulator (Nexstim™, Helsinki, Finland) using a focal figure-of-eight bi-pulse 70 mm-coil while concomitantly recording EEG from a 60 channels cap. The stimulation target was the left PPC, between P1 and CP1 EEG electrodes.

Coil positioning and monitoring throughout recordings were achieved using a Navigated Brain Stimulation (NBS) system (Nexstim™, Helsinki, Finland) on the individual high-resolution (1 × 1 × 1 mm) structural MRI. The MRIs were previously acquired for each participant using a 3T Intera Philips body scanner (Philips Medical Systems, Best, NL). The coil was placed tangentially to the scalp. The position was adjusted for each participant to direct the electric field perpendicularly to the shape of the cortical gyrus, following the same procedure used in previous studies (Casarotto et al., 2010; Mattavelli et al., 2013; Romero Lauro et al., 2014) (see Fig. 4– Panel a for a graphical representation).

The NBS system allows estimating online the intensity (V/m) of the intracranial electric field induced by the TMS pulses at the stimulation hotspot, taking into consideration anatomical features of each participant such as head and brain shape, cortex distance from the scalp and coil position. Before each session, we ran a short preliminary TMS-EEG recording including 20–30 trials (see for recent recommendations Hernandez-Pavon et al., 2023) to inspect in real-time that pulses did not elicit muscular activity or other TMS artifacts (Mutanen et al., 2013). In the preliminary recording, we started from an estimated electrical induced field of 90 V/m. We increased TMS intensity to reach a peak-to-peak amplitude of average TEPs ~ 10 μV (Casarotto et al., 2022). The average stimulation intensity, expressed as a percentage of the maximal output of the stimulator, was 64% (range = 60 - 73%), corresponding to an electric field of 105 ± 12 V/m, in line with our previous studies targeting the same region (Romero Lauro et al., 2014; Varoli et al., 2018). TEPs were recorded using single TMS pulses on the left PPC. Each recording session lasted about 7 min, during which 180 pulses were delivered, with an inter-stimulus interval (ISI) randomly jittered between 2000 and 2300 ms (0.4 – 0.5 Hz). During TMS-EEG registration, participants fixated on a white cross on a black screen (17″). Participants heard a noise-masking trace during the TMS-EEG recording, to avoid the presence of auditory artifacts (Casarotto et al., 2010).

3.1.5. TMS-EEG data preprocessing

EEG data preprocessing was performed with Matlab R2016b (Mathworks, Natick, MA, USA). First, recordings were down-sampled to 725 Hz. The continuous signal was split into single trials, from 800 ms before to 800 ms after the TMS pulse. Trials with artifacts due to eye blink/movements or spontaneous muscle activity were removed following a semiautomatic procedure (Casali et al., 2010) and the visual inspection of the signal by trained experimenters. TEPs were computed by averaging selected artifact-free single trials and filtering them between 2 and 40 Hz. Bad or missing channels, such as P2 and CP2 that were right above the cathode were interpolated using the spherical interpolation function of EEGLAB (Delorme and Makeig, 2004). TEPs were then average-referenced, and baseline corrected between −300 and −50 ms before the TMS pulse. The average number of trials considered in the analysis was 122 (SD = ± 4) for the pre-tDCS and 120 (SD = ± 2) for the post-tDCS condition.

3.1.6. TMS-EEG data analyses

We performed three analyses on our EEG dataset for c-tDCS and sham conditions. Two analyses were performed at the sensors level: Global and Local Mean Field Power (GMFP, LMFP) computation and cluster analysis. GMFP and LMFP were computed as indexes of global and local

excitability to mirror the analyses run in our previous studies in which a- and c-tDCS were delivered at resting state (Romero Lauro et al., 2014, 2016; Varoli et al., 2018). We added the cluster analysis to avoid the selection of a priori time windows and regions of interest. The third analysis was performed at the level of cortical sources, to avoid the potential confound of volume conduction, which is even more relevant with the delivery of tDCS (Bailey et al., 2016), and to achieve a better definition of the spatial distribution of the tDCS effects (Casarotto et al., 2010; Romero Lauro et al., 2016). For the sake of brevity, here we report the procedures and results of the Cluster analysis and source analysis. Details about the procedures and the results of GMFP and LMFP can be found in Supplementary Materials (Section C).

3.1.6.1. Cluster analysis. For both cathodal and sham conditions, the pre- and post-tDCS sessions were compared through a cluster-based permutation test (Maris and Oostenveld, 2007) implemented in the "FieldTrip" MATLAB toolbox for M/EEG analysis (Oostenveld et al., 2011). This procedure solves the multiple comparisons problem by permuting and clustering data based on temporal and spatial proximity. More precisely, a big number of N of data permutations are performed by shuffling the labels of the experimental conditions. Then t-tests are computed at each time point for each permutation. All samples with a statistic corresponding to a p-value smaller than 0.05 are thus clustered based on spatial proximity. Cluster-level statistics are calculated by taking the sum of the t-values within each cluster. Finally, the cluster-corrected threshold is computed as the maximum cluster-level statistics permutation distribution (Maris and Oostenveld, 2007). In these analyses, 10,000 permutations were performed for each comparison with a permutation-significance level of $p = .05$ for the time window between 0 and 300 ms from the TMS onset. We chose this interval after observing the presence of relevant peaks in the butterfly plots, which occurred, as usual, in the first 300 ms (Casarotto et al., 2010).

3.1.6.2. Source analysis. As the first step, individual standardized meshes were reconstructed for each participant starting from their structural MRIs (SPM8) (Ashburner et al., 2011). We obtained meshes of cortex, skull, and scalp compartments (containing 3004, 2000, and 2000 vertices, respectively), normalized to the MNI atlas. Then, the EEG sensor's position was aligned to the canonical anatomical markers (pre-auricular points and nasion) for each participant, and the forward model was computed. The inverse solution was calculated on the average of all artifact-free TMS-EEG trials, using the weighted minimum norm estimate with a smoothness prior, following the same procedures as in Casali and colleagues (Casali et al., 2010). After source reconstruction, a statistical threshold was computed to assess when and where the post-TMS cortical response differed from pre-TMS activity. We applied a non-parametric permutation-based procedure (Pantazis et al., 2003). We obtained a binary spatial-temporal distribution of statistically significant sources, including only information from significant cortical sources in further analyses. As a measure of global cortical activation, we cumulated the absolute significant current density (global SCD, measured in $\mu A/mm^2$) (Casali et al., 2010) (overall 3004 cortical vertexes) for each recording session (pre-tDCS, post-tDCS). To mirror the LMFP at the sensors level, we computed a local SCD in the vertexes within four different Brodmann's areas (BAs), identified using an automatic tool of anatomical classification (WFUPickAtlas tool, http://www.ansir.wfubmc.edu). These BAs corresponded to the original four clusters of LMFP (left/right BA6 and 7).

To coherently perform the analysis at the level of the sources, we started with the sensor cluster analysis results. The global SCD and local SCD were then computed in the time window from 180 to 230 ms, in which the significant cluster was found. On this data, a linear mixed model with the factor *recording session* (2 levels: pre-tDCS vs. post-tDCS) was run for Global SCD and the four regions of interest ROIs (left and right BA7 and BA6). We used the same analyses and procedures to analyze data from sham sessions.

3.2. Results

3.2.1. Behavioral results

Behavioral data were analyzed following the same procedure described in Experiment 1. Details of model selection are reported in the Supplementary materials (Section C).

MPCT statistical analyses were performed on 3072 data points. The best-fitting model for the dependent variable accuracy included the simple effects of *trial order* and *trial validity* ($\chi^2_{(1)} = 5.6$, $p = .018$) (see Table S6 for the model selection). Considering the *trial order* effect ($\chi^2_{(1)} = 5.7$, $p = .017$), participants became progressively less accurate in the mPCT performance, suggesting an effect of fatigue during task execution. Concerning *trial validity* ($\chi^2_{(1)} = 13.4$, $p < .001$), as expected participants' accuracy was higher in the valid vs. invalid condition. Relatively to RTs, we considered only accurate responses, and analyses included 3014 data points. The best-fitting model comprised the simple effects of *trial order* and *tDCS condition* ($\chi^2_{(1)} = 34.4$, $p = < 0.001$) (see Table S7 for details on model selection). Considering the effect of *trial order* ($\chi^2_{(1)} = 34.6$, $p < .001$), participants became faster while performing the task, showing an effect of learning on the performance speed. Relatively to the *tDCS condition* ($\chi^2_{(1)} = 9.6$, $p = .002$), RTs were slower during the cathodal as compared to the sham stimulation (see Fig. 5 for a graphical representation). Considering the VWMT, statistical analyses were performed on 64 data points. The results showed no significant main effects or interaction between the *tDCS condition* and *attended hemifield* (see Table S8 for details on model selection).

3.2.2. TMS-EEG data

We here report the results of cluster and source analysis. Results of GMPF and LMFP can be found in the Supplementary materials (Section C).

3.2.2.1. Cathodal stimulation - cluster analysis. A cluster-based analysis evaluating the effect of tDCS stimulation on the recording session (Pre-tDCS vs. Post-tDCS) revealed a significant positive cluster ($p = .023$; Pre > Post) in frontoparietal electrodes in a time range from 180 to 230 ms from the TMS onset. TEPs' scalp topographies of statistically significant differences showed that the positive cluster was associated with frontocentral electrodes and covered a bilateral portion of brain regions.

3.2.2.2. Cathodal stimulation - source modeling analyses. Source modeling analyses performed in the cluster analysis' significant time window confirmed results from the cluster analysis at the sensors level. The best-fitted model on the index of global cortical activation, namely Global SCD, included the main effect *recording session* ($\chi^2_{(2)} = 6.4$; $p = .014$) with a decrease of TEPs amplitude after tDCS stimulation (see Fig. 7). Similarly, in the analysis for the Local SCD computed for 4 BAs, namely bilateral BA6 and BA7, the factor *recording session* was included in the final model as the main effect for left BA7 ($\chi^2_{(2)} = 5.87$; $p = .015$), right BA7 ($\chi^2_{(2)} = 6.0$; $p = .014$) and left BA6 ($\chi^2_{(2)} = 7.9$; $p = .005$). Only for the right BA6 no effect of real c-tDCS was highlighted on local SCD ($\chi^2_{(2)} = 1.5$; $p = .224$).

3.2.2.3. Sham stimulation - cluster analysis. For the sham stimulation condition, the results revealed neither positive nor negative significant clusters (Fig. 6).

3.2.2.4. Sham stimulation - source modeling analyses. We decided to perform the Source modeling analysis to explore at a different signal level, although no significant results were found at the sensors level with cluster permutation. For this reason, the Source modeling analyses were performed between 180 and 230 ms, which is the significant time window for c-tDCS. The sham data lacked statistically significant effects, confirming the results of the sensor analyses, but at a global level only. The Global SCD final model did not include *recording session* ($\chi^2_{(2)} = 0.13$;

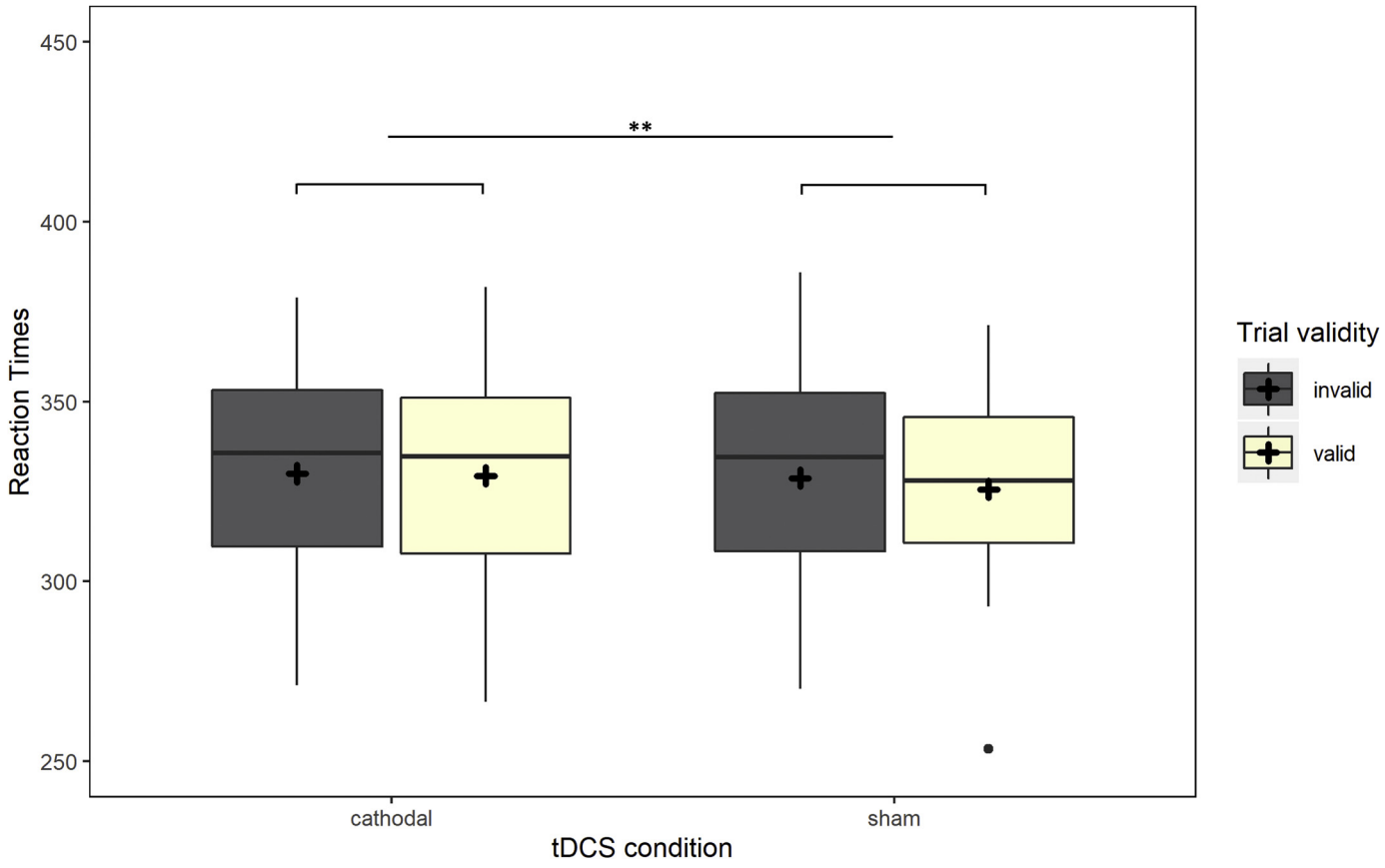

Fig. 5. Behavioral results of mPCT in Experiment 2. The boxplots represent the RTs data for the valid (light yellow boxes) and invalid (dark gray boxes) trial conditions in the c- and sham tDCS sessions, on the left and the right, respectively. Asterisks represent statistical p-values *** $p < .001$. ** $p < .01$, * $p < .05$.

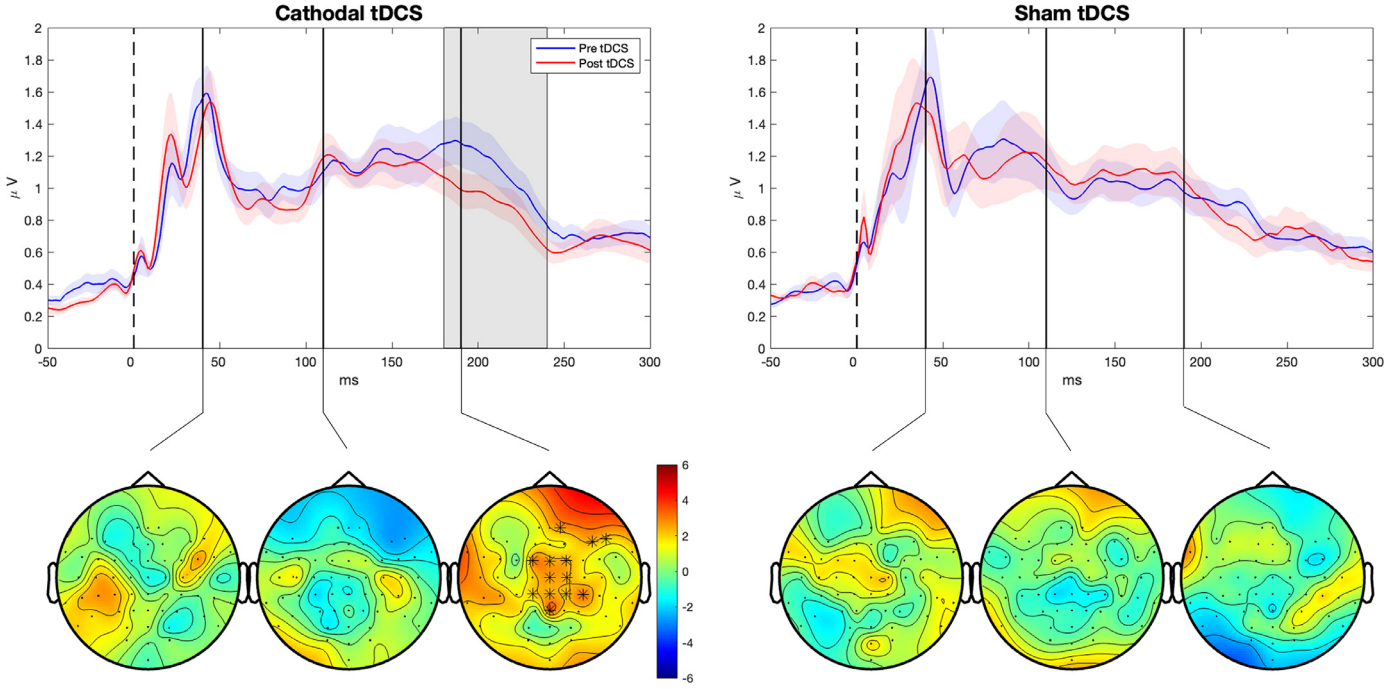

Fig. 6. Results of cluster analysis. The upper row shows the Grand Average of GMFP computed by averaging the GMFPs calculated for each subject in the Pre-tDCS (blue line ± SE) and Post-tDCS (red line ± SE) recording sessions for cathodal (left) and sham (right) conditions. The gray bars define the time window where cluster analysis evidenced significant results. The lower row represents the mean topographies of the results of the cluster analysis computed in correspondence with GMFP maxima for pre-tDCS recordings, highlighting the significant clusters. The mean topographies at the same time points are represented also for the Sham condition.

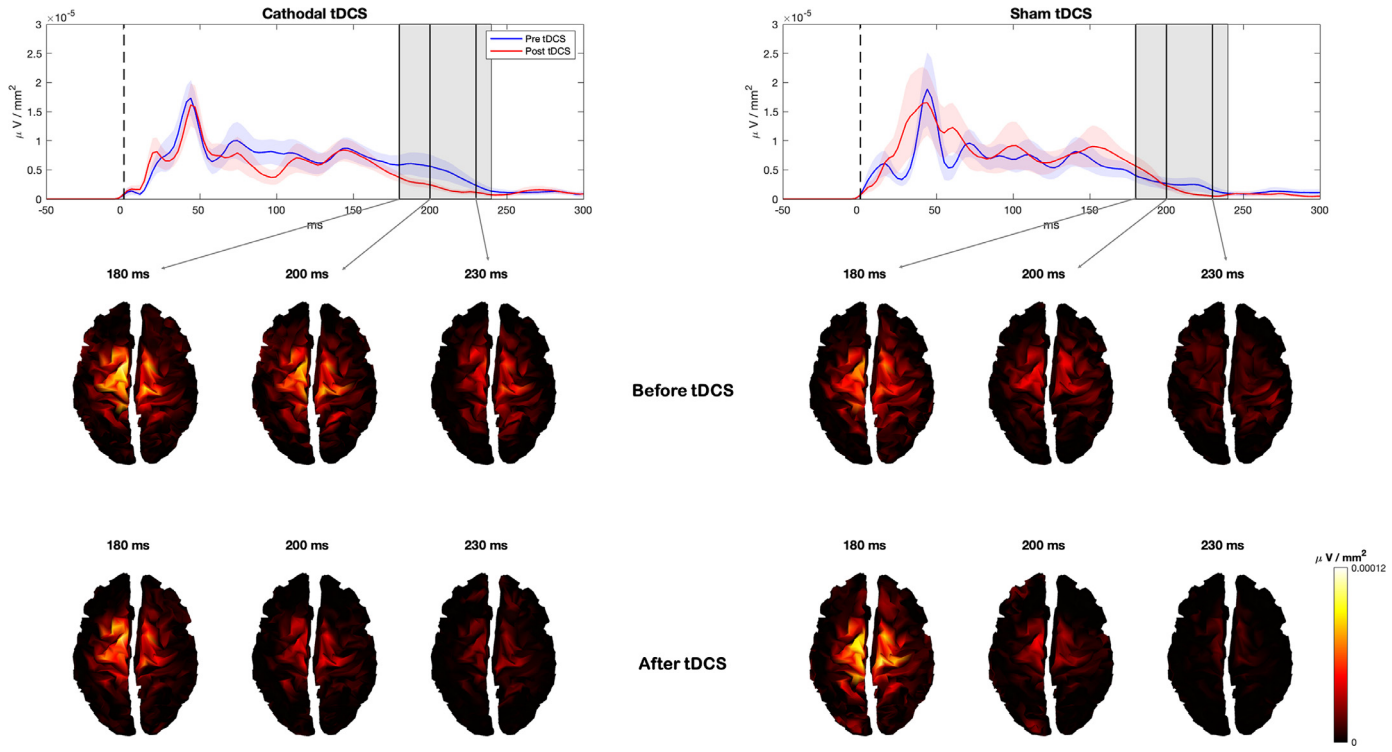

Fig. 7. Active vertexes and current spread at the local maxima in the TEPs time windows were revealed by the cluster analysis for both cathodal and sham tDCS. For each recording session (pre-and post-tDCS), the GMFP is shown on the first top row. The gray bars define the time window where cluster analysis evidenced significant results. The second and third rows show the estimated cortical sources in time coincidence with the maximum GMFP value, between 180 and 230 ms.

p = .711), indicating no effect of sham stimulation on cortical excitability (see Fig. 7).

The same holds for both left ($\chi^2_{(2)}$ = 0.03; p = .850) and right ($\chi^2_{(2)}$ = 0.15; p = .708) BA7, as well as for left BA6 ($\chi^2_{(2)}$ = 0.56; p = .450), where LRT indicated no inclusion of the factor *recording session* in the final model. Different from what emerged for sensors data, at the level of the sources, the main effect of the *recording session* was significant ($\chi^2_{(2)}$ = 5.19; p = .022) for the right BA6. Results in this area showed wider TEPs after sham stimulation than those before.

Finally, as in a previous study by Pisoni et al. (Pisoni et al., 2018), we investigated possible links between cognitive and neurophysiological measures by computing correlations between the real vs. sham differences in the mPCT performance (RTs) and cortical excitability. Results did not highlight significant correlations between changes in excitability and behavioral performance (ps > 0.204) (see Supplementary materials - Figure S4 for a graphical representation of the correlations pattern).

3.3. Interim comment

Regarding the behavioral results, we confirmed that c-tDCS over rPPC modulated the performance at mPCT and not VWMT. We partially replicated the behavioral effects in mPCT observed in Experiment 1 since in Experiment 2 c-tDCS slowed down the RTs compared to sham stimulation independently from the trial validity. Crucially, at a neurophysiological level, cluster analysis and source analysis converged in showing that c-tDCS reduced cortical excitability in the time window of 180–230 ms from TMS onset in a frontoparietal network.

4. General discussion

The present study investigated the behavioral and neurophysiological effects of c-tDCS delivered over rPPC during the performance of two visuospatial tasks.

Concerning behavioral effects, the results of Experiments 1 and 2 converged in showing that c-tDCS on rPPC modulated proficiency in the mPCT. Critically, in Experiment 1, c-tDCS eliminated the advantage for RTs in the valid cue condition since no difference was found between valid and invalid cues, as observed in the sham condition and in the pilot study. These results suggest that tDCS operates in reducing the pre-allocation of attention elicited by an exogenous cue. In Experiment 2, a significant increment of RTs in the mPCT during c-tDCS was found compared to the sham condition. Previous studies investigating tDCS effects on visuospatial attention showed mixed results, thus providing inconclusive findings (Demartini et al., 2019; Li et al., 2015a; Lo et al., 2019; Roy et al., 2015). It is possible that methodological differences, such as montage, polarity, and timing of stimulation, accounted for this heterogeneity in results. C-tDCS did not impact performance on the VWMT, either in Experiment 1 or 2. Also in this case, previous results were heterogeneous, with some studies highlighting a modulatory tDCS effect in this domain, and others not (Heimrath et al., 2012; Hill et al., 2016; Robison et al., 2017; Tseng et al., 2012). Results inconsistency has been previously related to the strategies employed in the task execution, which largely depend on the individual WM capacity (Heinen et al., 2016; Jones and Berryhill, 2012; Li et al., 2017).

Concerning the neurophysiological data, the cluster analysis at the sensor level revealed a significantly different bilateral frontoparietal positivity comparing pre- and post-c-tDCS, between 180 and 230 ms from the TMS onset: cortical excitability decreased after c-tDCS compared to the pre-stimulation recording. Source modeling analysis confirmed the cluster analysis results. Indeed, SCD changed after stimulation compared to the pre-tDCS condition when it was computed at a global level and in three of the four BAs. Computing the data in the time window derived from the cluster analysis (180 – 230 ms), a significant change was found bilaterally for BA7 and left BA6, but not for right BA6.

In a previous study (Varoli et al., 2018), we failed to observe any changes in cortical excitability when c-tDCS was delivered at rest. Since

in this previous study the analyses were performed only in the first 150 ms of TEPs, to rule out that the absence of neurophysiological effects might depend upon a too short time window of interest, the same cluster analysis performed in the present study was also run on the previously collected dataset. Crucially no significant positive or negative clusters were found in the re-analysis.

Combined with our previous study (Varoli et al., 2018), we here provide clear-cut evidence that, when stimulation is cathodal, state dependence is crucial to effectively modulate human cortical excitability outside the corticospinal domain. It can be argued, indeed, that c-tDCS - which should reduce the level of neural discharge - may produce effects only in systems with a high level of basal activity, as that elicited by concurrent task execution. It is possible that c-tDCS may have little or no effect at the resting state because only low levels of spontaneous discharge occur. A possible explanation could be the crucial role played in tDCS effects by the location and frequency of active synapses, as suggested by in vitro modeling (Lafon et al., 2017). The state-dependent effectiveness for neurophysiological modulation that we observed might be strictly connected to the long-lasting plastic changes induced in the stimulated area by the concurrent task execution.

The role of state-dependency for c-tDCS neurophysiological effects might provide novel insights into the mechanism underlying anodal vs. cathodal imbalance. Notwithstanding the increasing evidence on the state-dependency of NiBS effects, indeed, there is still inconsistency in the literature about the application of tDCS during a task. Many scholars prefer to use tDCS as priming – namely at rest and before performing a task. The often-reported null effects of c-tDCS might then depend on the frequency of offline paradigms. Jacobson et al. (2012) systematically explored the factors underlying anodal vs. cathodal imbalance of effects and proposed that a relevant role is played by the motor vs. cognitive targeted function, being the likelihood of achieving anodal-excitatory vs. cathodal-inhibitory effects higher in the former and reduced in the second (they also clarified that in the cognitive domain usually there is a significantly higher chance to observe an excitatory effect of anodal whereas a lower probability of observing an inhibitory effect of c-tDCS, usually leading to null results). Interestingly, they also checked whether several stimulation parameters, likewise the intensity, duration, and electrodes size, might affect such imbalance, without finding any significant result. However, they did not consider the role of the online vs. offline paradigm, i.e., whether the stimulation was applied at rest or before vs. during a task. Our data suggest that the status of activation of the stimulated brain area might affect such imbalance, and the prediction would be that a lower imbalance can be found in online paradigms. Future studies might further test this hypothesis.

Notably, the neurophysiological c-tDCS effects seem to be restricted to those areas activated by the task execution, as previously observed for a-tDCS (Pisoni et al., 2018). Different studies have indeed shown that a dorsal frontoparietal network is globally associated with attention orientation, even if the regions in the system are engaged differently over time and across the hemispheres concerning the type of attention (Chica et al., 2013). Within this framework, attentional performance critically depends on the interaction between PPC and the frontal eye fields, one holding the sensory representation, and the other holding a motor representation (Mesulam, 1981; Torriero et al., 2019). In line with our results, Thiel et al. (Thiel et al., 2004) showed that the specific reorienting attention activity in PCT increased activation in a bilateral frontoparietal network, including left and right intraparietal sulci, right temporoparietal junction, and left and right middle frontal gyri in healthy volunteers. Our study found a decreased cortical excitability in the left but not in the right frontal area. Although frontal and parietal lesions can both induce neglect (Halligan et al., 2003), there is some divergence in imaging and patients data concerning the role of the frontal cortex in reorienting attention since some frontal patients did not show specific deficits in these types of tasks (Petersen et al., 1989; Posner et al., 1987). However, another not mutually exclusive hypothesis related to the reported left frontal decrease in cortical excitability should be considered. Indeed, in our montage, the 'anode' was placed over the left supraorbital region. Although we used different size electrodes to increase stimulation focality (Nitsche et al., 2008), it is possible that the anode was still inducing changes in brain excitability. Following this reasoning, the decrease in excitability in the left prefrontal cortex ten minutes after the end of stimulation can be considered as a 'return' or 'opponent' current that follows the previous depolarization induced by the anode, thus suggesting a homeostatic reaction of the brain (e.g., Fertonani and Miniussi, 2017). To further clarify this point, future studies should compare different bi-cephalic and extra-cephalic electrodes configurations (e.g., Accornero et al., 2014). Considering this hypothesis also related to the mPCT performance, it is possible that the reported behavioral findings could be induced by the specific electrodes configuration used in the present experiment. Indeed, we know that visuospatial attention is supported by a frontoparietal network (Corbetta et al., 2008; Li et al., 2015a). However, disentangling between the effects of the anode and the cathode to explore the neural underpinnings of visuospatial attention is beyond the aims of our project. Indeed, the task choice in the present work was related to the involvement of the parietal cortex in its execution since we wanted to compare the effect on brain excitability of c-tDCS delivered with a concurrent task with our previous study in which c-tDCS was delivered at the resting-state (Varoli et al., 2018), with a larger interest on state-dependency than on neural bases supporting visuospatial processing.

The occurrence of neurophysiological effects in task-relevant brain areas supports the activity-selectivity hypothesis, according to which functional tDCS specificity may derive from either active neuronal networks that are preferentially modulated by tDCS or from input-selectivity, where a bias is applied to different synaptic inputs (Bikson and Rahman, 2013).

Regarding the timing at which the neurophysiological effects of the stimulation were observed, c-tDCS affected cortical excitability at a relatively later stage. Whereas early TEPs are considered a direct and reliable marker of cortical excitability of the targeted area (Ilmoniemi and Kičić, 2010; Pellicciari et al., 2013), the middle-latency component reflects the connectivity of the functional network activated by the task (Casarotto et al., 2010; Casula et al., 2022; Ilmoniemi and Kičić, 2010; Pisoni et al., 2018; Veniero et al., 2011). The timing of neurophysiological effects might then suggest that rather than local excitability, c-tDCS affected the connectivity within the frontoparietal network underlying the attentional process required by mPCT.

Crucially, no significant changes in cortical excitability were found when sham stimulation was delivered. The only exception was at the level of the sources where, only in correspondence with the right BA6, we found an increase in SCD in the post- compared to pre-tDCS condition. What occurs in the sham control condition can be considered a baseline, reflecting modulations possibly due to the task execution. Therefore, the significant increase of SCD in the right BA6 after sham may be attributed to the involvement of this area in the visuospatial orienting attention (Brovelli et al., 2005; Nobre et al., 2000). Consequently, the lack of effect on right BA6 after c-tDCS can be interpreted as an effect of the stimulation: c-tDCS might have reduced cortical excitability in this area, canceling the activation effect due to the task execution observed in the sham condition. It could be possible that the right BA6 plays a peculiar role in the excitability-inhibitory processes in the network. This area could compensate for the destructive effects of c-tDCS on the other regions in the system during task execution. Further studies need to be performed to disentangle this issue.

4.1. Limitations of the present research

Regarding the limitations of the present research, a main issue is that we did not run an a priori power analysis for Experiment 2; instead, we based sample size decision on previous studies from our and other research groups using TMS-EEG to disentangle real vs. sham tDCS effects in between (e.g., Grasso et al., 2021) and within (Hill et al., 2018;

Romero Lauro et al., 2014) experimental designs. We acknowledge that our sample size is unpowered for the tDCS effect on task performance (Minarik et al., 2016), thus preventing us from firmly confirming the behavioral effects observed in Experiment 1. Future research is then needed to further explore the role of rPPC in visuospatial attentional tasks. As a second limitation, for sham tDCS, we used standard blinding procedures that have been reported to be effective at an intensity of 1 mA (Gandiga et al., 2006; Poreisz et al., 2007; Ambrus et al., 2012; Woods et al., 2016; Mattavelli et al., 2022). However, we did not check for the participants' discomfort sensations or guessing of the stimulation condition in our sample.

As a last point, we did not check for nicotine consumption among our participants. Despite international safety and recommendations guidelines for NiBS administration (Antal et al., 2017; Hernandez-Pavon et al., 2023; Rossi et al., 2021) do not consider smoking among the exclusion criteria for tDCS/TMS-EEG/TMS delivery within healthy individuals, we acknowledge the importance of checking for this variable that could influence tDCS-induced plasticity (Grundey et al., 2013; see Vergallito et al., 2022 for a recent review). Therefore, in our future research, we will consider this issue more carefully, administering structured checklists (e.g., Antal et al., 2017).

4.2. Conclusions

To conclude, our results shed light on the dependence of tDCS effects on the state of activity of the stimulated regions. Supporting previous evidence for a-tDCS (Pisoni et al., 2018), the present findings showed that delivering c-tDCS during a task would confine the neurophysiological effect on the task-relevant areas, thus accounting for the specificity of the behavioral impact usually observed. In the case of c-tDCS, at least for parietal cortex stimulation, the concurrent task activity seems essential to observe cortical excitability modulations. The possibilities of translating this knowledge into a clinical domain are promising, considering that neurological and psychiatric conditions are characterized by the presence of a pathologically altered neural plasticity and connectivity, that could be restored by combining brain stimulation with concurrent cognitive tasks, training, or psychotherapy (Dedoncker et al., 2021; Sathappan et al., 2019; Tatti et al., 2022; Vergallito et al., 2021; Del Mauro et al., 2023).

Notably, the present findings are linked to the specific regions, tasks, and tDCS parameters used in the experiments. Future research should investigate whether the present conclusions can be generalized to other cognitive domains and brain networks.

Credit author statement

AV, EV, AP, GM, GV, and LJRL conceptualized the study; AV, EV, AP, GM, and LJRL further developed the methodology; EV, AP, GM, LDM, and SF collected the data which AV, EV, AP, GM, and LJRL analyzed. All the authors interpreted the results. AV, EV, and LJRL wrote the first version of the draft, which all the authors then revised. LJRL supervised all the experimental phases.

Open practices statement

The datasets generated and the script for the analyses is publicly available at https://osf.io/7jdmp/. The experiment was not preregistered.

Declaration of Competing Interest

None.

Data availability

I have shared the link of my data and code.

Supplementary materials

Supplementary material associated with this article can be found, in the online version, at doi:10.1016/j.neuroimage.2023.120242.

References

Accornero, N., Capozza, M., Pieroni, L., Pro, S., Davì, L., Mecarelli, O., 2014. EEG mean frequency changes in healthy subjects during prefrontal transcranial direct current stimulation. J. Neurophysiol. 112 (6), 1367–1375.

Ambrus, G.G., Al-Moyed, H., Chaieb, L., Sarp, L., Antal, A., Paulus, W., 2012. The fade-in–short stimulation–fade out approach to sham tDCS–reliable at 1 mA for naive and experienced subjects, but not investigators. Brain Stimul. 5 (4), 499–504.

Antal, A., Alekseichuk, I., Bikson, M., Brockmöller, J., Brunoni, A.R., Chen, R., … Paulus, W., 2017. Low intensity transcranial electric stimulation: safety, ethical, legal regulatory and application guidelines. Clin. Neurophysiol. 128 (9), 1774–1809.

Antal, A., Kincses, T.Z., Nitsche, M.A., Bartfai, O., Paulus, W., 2004. Excitability changes induced in the human primary visual cortex by transcranial direct current stimulation: direct electrophysiological evidence. Invest. Ophthalmol. Vis. Sci. 45 (2), 702e707.

Arif, Y., Spooner, R.K., Wiesman, A.I., Embury, C.M., Proskovec, A.L., Wilson, T.W., 2020. Modulation of attention networks serving reorientation in healthy aging. Aging (Albany NY) 12 (13), 12582.

Ashburner, J., Barnes, G., Chen, C., 2011. Functional imaging laboratory: wellcome trust centre for neuroimaging. SPM8 Manual *London, UK*.

Baayen, R., 2008. Analyzing Linguistic Data: A Practical Introduction to Statistics using R. Cambridge University Press, Cambridge.

Baayen, R.H., Milin, P., 2010. Analyzing reaction times. Int. J. Psychol. Res. (Medellin) 3 (2), 12–28.

Baayen, R.H., Davidson, D.J., Bates, D.M., 2008. Mixed-effects modeling with crossed random effects for subjects and items. J. Mem. Lang. 59 (4), 390–412.

Bailey, N.W., Thomson, R.H., Hoy, K.E., Hernandez-Pavon, J.C., Fitzgerald, P.B., 2016. TDCS increases cortical excitability: direct evidence from TMS-EEG. Cortex 74, 320–322.

Bates, D., Maechler, M., Bolker, B., & Walker, S. (2015). *lme4: Linear mixed-effects models using Eigen and S4. R package version 1.1–7. 2014*.

Batsikadze, G., Moliadze, V., Paulus, W., Kuo, M.F., Nitsche, M., 2013. Partially non-linear stimulation intensity-dependent effects of direct current stimulation on motor cortex excitability in humans. J. Physiol. (Lond.) 591 (7), 1987–2000.

Behrmann, M., Geng, J.J., Shomstein, S., 2004. Parietal cortex and attention. Curr. Opin. Neurobiol. 14 (2), 212–217.

Berryhill, M.E., Martin, D., 2018. Cognitive effects of transcranial direct current stimulation in healthy and clinical populations: an overview. J. ECT 34 (3), e25–e35.

Bikson, M., Rahman, A., 2013. Origins of specificity during tDCS: anatomical, activity-selective, and input-bias mechanisms. Front. Hum. Neurosci. 7, 688.

Bindman, L.J., Lippold, O.C.J., Redfearn, J.W.T., 1964. The action of brief polarizing currents on the cerebral cortex of the rat (1) during current flow and (2) in the production of long-lasting after-effects. J. Physiol. (Lond.) 172 (3), 369–382.

Bocci, T., Ferrucci, R., Priori, A., 2020. Neurophysiological Bases and Mechanisms of Action of Transcranial Direct Current Stimulation (tDCS). In: Non Invasive Brain Stimulation in Psychiatry and Clinical Neurosciences. Springer, pp. 19–29.

Boggio, P.S., Rigonatti, S.P., Ribeiro, R.B., Myczkowski, M.L., Nitsche, M.A., Pascual-Leone, A., Fregni, F., 2008. A randomized, double-blind clinical trial on the efficacy of cortical direct current stimulation for the treatment of major depression. Int. J. Neuropsychopharmacolog. 11 (2), 249–254.

Bortoletto, M., Pellicciari, M. C., Rodella, C., Miniussi, C., 2015. The interaction with task-induced activity is more important than polarization: a tDCS study. Brain Stimul. 8 (2), 269–276.

Bradley, C., Nydam, A.S., Dux, P.E., Mattingley, J.B., 2022. State-dependent effects of neural stimulation on brain function and cognition. Nat. Rev. Neurosci. 1–17.

Brovelli, A., Lachaux, J.-P., Kahane, P., Boussaoud, D., 2005. High gamma frequency oscillatory activity dissociates attention from intention in the human premotor cortex. Neuroimage 28 (1), 154–164.

Cambiaghi, M., Velikova, S., Gonzalez-Rosa, J.J., Cursi, M., Comi, G., Leocani, L., 2010. Brain transcranial direct current stimulation modulates motor excitability in mice. Eur. J. Neurosci. 31 (4), 704–709.

Casali, A.G., Casarotto, S., Rosanova, M., Mariotti, M., Massimini, M., 2010. General indices to characterize the electrical response of the cerebral cortex to TMS. Neuroimage 49 (2), 1459–1468.

Casarotto, S., Fecchio, M., Rosanova, M., Varone, G., D'Ambrosio, S., Sarasso, S., … Massimini, M, 2022. The rt-TEP tool: real-time visualization of TMS-Evoked Potentials to maximize cortical activation and minimize artifacts. J. Neurosci. Method. 370, 109486.

Casarotto, S., Lauro, L.J.R., Bellina, V., Casali, A.G., Rosanova, M., Pigorini, A., … Massimini, M., 2010. EEG responses to TMS are sensitive to changes in the perturbation parameters and repeatable over time. PLoS One 5 (4), e10281.

Casula, E.P., Tieri, G., Rocchi, L., Pezzetta, R., Maiella, M., Pavone, E.F., … Koch, G., 2022. Feeling of Ownership over an Embodied Avatar's Hand Brings About Fast Changes of Fronto-Parietal Cortical Dynamics. J. Neurosci. 42 (4), 692–701.

Chica, A.B., Bartolomeo, P., Lupiáñez, J., 2013. Two cognitive and neural systems for endogenous and exogenous spatial attention. Behav. Brain Res. 237, 107–123.

Corbetta, M., Shulman, G.L., 2002. Control of goal-directed and stimulus-driven attention in the brain. Nat. Rev. Neurosci. 3 (3), 201–215.

Corbetta, M., Kincade, J.M., Ollinger, J.M., McAvoy, M.P., Shulman, G.L., 2000. Voluntary orienting is dissociated from target detection in human posterior parietal cortex. Nat. Neurosci. 3 (3), 292–297.

Corbetta, M., Patel, G., Shulman, G.L., 2008. The reorienting system of the human brain: from environment to theory of mind. Neuron 58 (3), 306–324.

Cowan, N., 2001. The magical number 4 in short-term memory: a reconsideration of mental storage capacity. Behav. Brain Sci. 24 (1), 87–114.

Creutzfeldt, O.D., Fromm, G.H., Kapp, H., 1962. Influence of transcortical dc currents on cortical neuronal activity. Exp. Neurol. 5 (6), 436–452.

Dedoncker, J., Baeken, C., De Raedt, R., Vanderhasselt, M.-A., 2021. Combined transcranial direct current stimulation and psychological interventions: state of the art and promising perspectives for clinical psychology. Biol. Psychol. 158, 107991.

Dedoncker, J., Brunoni, A.R., Baeken, C., Vanderhasselt, M.-A., 2016. A systematic review and meta-analysis of the effects of transcranial direct current stimulation (tDCS) over the dorsolateral prefrontal cortex in healthy and neuropsychiatric samples: influence of stimulation parameters. Brain Stimul. 9 (4), 501–517.

Del Mauro, L., Vergallito, A., Gattavara, G., Juris, L., Gallucci, A., Vedani, A., … Romero Lauro, L.J., 2023. Betting on non-invasive brain stimulation to treat gambling disorder: a systematic review and meta-analysis. Brain Sci. 13 (4), 698.

Delorme, A., Makeig, S., 2004. EEGLAB: an open source toolbox for analysis of single-trial EEG dynamics including independent component analysis. J. Neurosci. Methods 134 (1), 9–21.

Demartini, B., Volpe, R., Mattavelli, G., Goeta, D., D'Agostino, A., Gambini, O, 2019. The neuromodulatory effect of tDCS in patients affected by functional motor symptoms: an exploratory study. Neurolog. Sci. 40 (9), 1821–1827.

Faul, F., Erdfelder, E., Lang, A.G., Buchner, A., 2007. G* Power 3: a flexible statistical power analysis program for the social, behavioral, and biomedical sciences. Behav. Res. Method. 39 (2), 175–191.

Fertonani, A., Miniussi, C., 2017. Transcranial electrical stimulation: what we know and do not know about mechanisms. Neuroscientist 23 (2), 109–123.

Fregni, F., El-Hagrassy, M.M., Pacheco-Barrios, K., Carvalho, S., Leite, J., Simis, M., … Venkatasubramanian, G., 2020. Evidence-based guidelines and secondary meta-analysis for the use of transcranial direct current stimulation (tDCS) in neurological and psychiatric disorders. Int. J. Neuropsychopharmacolog..

Friedman, H.R., Goldman-Rakic, P.S., 1994. Coactivation of prefrontal cortex and inferior parietal cortex in working memory tasks revealed by 2DG functional mapping in the rhesus monkey. J. Neurosci. 14 (5), 2775–2788.

Fritsch, B., Reis, J., Martinowich, K., Schambra, H.M., Ji, Y., Cohen, L.G., Lu, B., 2010. Direct current stimulation promotes BDNF-dependent synaptic plasticity: potential implications for motor learning. Neuron 66 (2), 198–204.

Gandiga, P. C., Hummel, F. C., Cohen, L. G., 2006. Transcranial DC stimulation (tDCS): a tool for double-blind sham-controlled clinical studies in brain stimulation. Clin. Neurophysiol. 117 (4), 845–850.

Gelman, A., Hill, J., 2006. Data Analysis Using Regression and Multilevel/Hierarchical Models. Cambridge university press.

Grasso, P.A., Tonolli, E., Bortoletto, M., Miniussi, C., 2021. tDCS over posterior parietal cortex increases cortical excitability but decreases learning: an ERPs and TMS-EEG study. Brain Res. 1753, 147227.

Grundey, J., Freznosa, S., Klinker, F., Lang, N., Paulus, W., Nitsche, M.A., 2013. Cortical excitability in smoking and not smoking individuals with and without nicotine. Psychopharmacol. (Berl.) 229 (4), 653–664. doi:10.1007/s00213-013-3125-6.

Halligan, P.W., Fink, G.R., Marshall, J.C., Vallar, G., 2003. Spatial cognition: evidence from visual neglect. Trend. Cogn. Sci. (Regul. Ed.) 7 (3), 125–133.

Hassanzahraee, M., Nitsche, M.A., Zoghi, M., et al., 2020. Determination of anodal tDCS intensity threshold for reversal of corticospinal excitability: an investigation for induction of counter-regulatory mechanisms. Sci. Rep. 10, 16108.

Heimrath, K., Sandmann, P., Becke, A., Müller, N.G., Zaehle, T., 2012. Behavioral and electrophysiological effects of transcranial direct current stimulation of the parietal cortex in a visuo-spatial working memory task. Front. Psychiatry 3, 56.

Heinen, K., Sagliano, L., Candini, M., Husain, M., Cappelletti, M., Zokaei, N., 2016. Cathodal transcranial direct current stimulation over posterior parietal cortex enhances distinct aspects of visual working memory. Neuropsychologia 87, 35–42.

Hernandez-Pavon, J.C., Veniero, D., Bergmann, T.O., Belardinelli, P., Bortoletto, M., Casarotto, S., … Ilmoniemi, R.J., 2023. TMS combined with EEG: recommendations and open issues for data collection and analysis. Brain Stimul. 16, 567–593.

Hill, A.T., Fitzgerald, P.B., Hoy, K.E., 2016. Effects of anodal transcranial direct current stimulation on working memory: a systematic review and meta-analysis of findings from healthy and neuropsychiatric populations. Brain Stimul. 9 (2), 197–208.

Hill, A.T., Rogasch, N.C., Fitzgerald, P.B., Hoy, K.E., 2018. Effects of single versus dual-site High-Definition transcranial direct current stimulation (HD-tDCS) on cortical reactivity and working memory performance in healthy subjects. Brain Stimul. 11 (5), 1033–1043.

Ilmoniemi, R.J., Kičić, D., 2010. Methodology for combined TMS and EEG. Brain Topogr. 22 (4), 233–248.

Jacobson, L., Koslowsky, M., Lavidor, M., 2012. tDCS polarity effects in motor and cognitive domains: a meta-analytical review. Exp. Brain Res. 216 (1), 1–10.

Jones, K.T., Berryhill, M., 2012. Parietal contributions to visual working memory depend on task difficulty. Front. Psychiatry 3, 81.

Juan, C.-H., Tseng, P., Hsu, T.-Y., 2017. Elucidating and modulating the neural correlates of visuospatial working memory via noninvasive brain stimulation. Curr. Dir. Psychol. Sci. 26 (2), 165–173.

Lafon, B., Rahman, A., Bikson, M., Parra, L.C., 2017. Direct current stimulation alters neuronal input/output function. Brain Stimul. 10 (1), 36–45.

Li, L.M., Leech, R., Scott, G., Malhotra, P., Seemungal, B., Sharp, D.J., 2015a. The effect of oppositional parietal transcranial direct current stimulation on lateralized brain functions. Eur. J. Neurosci. 42 (11), 2904–2914.

Li, L.M., Uehara, K., Hanakawa, T., 2015b. The contribution of interindividual factors to variability of response in transcranial direct current stimulation studies. Front. Cell Neurosci. 9, 181.

Li, L.M., Violante, I.R., Leech, R., Ross, E., Hampshire, A., Opitz, A., … Sharp, D.J., 2019. Brain state and polarity dependent modulation of brain networks by transcranial direct current stimulation. Hum. Brain Mapp. 40 (3), 904–915.

Li, S., Cai, Y., Liu, J., Li, D., Feng, Z., Chen, C., Xue, G., 2017. Dissociated roles of the parietal and frontal cortices in the scope and control of attention during visual working memory. Neuroimage 149, 210–219.

Lo, O., van Donkelaar, P., Chou, L., 2019. Effects of transcranial direct current stimulation over right posterior parietal cortex on attention function in healthy young adults. Eur. J. Neurosci. 49 (12), 1623–1631.

Maris, E., Oostenveld, R., 2007. Nonparametric statistical testing of EEG-and MEG-data. J. Neurosci. Methods 164 (1), 177–190.

Martin, D.M., Liu, R., Alonzo, A., Green, M., Loo, C.K., 2014. Use of transcranial direct current stimulation (tDCS) to enhance cognitive training: effect of timing of stimulation. Exp. Brain Res. 232 (10), 3345–3351.

Matsunaga, K., Nitsche, M. A., Tsuji, S., Rothwell, J. C., 2004. Effect of transcranial DC sensorimotor cortex stimulation on somatosensory evoked potentials in humans. Clin. Neurophysiol. 115 (2), 456–460.

Mattavelli, G., Lo Presti, S., Tornaghi, D., Canessa, N., 2022. High-definition transcranial direct current stimulation of the dorsal anterior cingulate cortex modulates decision-making and executive control. Brain Struct. Funct. 227 (5), 1565–1576.

Mattavelli, G., Rosanova, M., Casali, A.G., Papagno, C., Lauro, L.J.R., 2013. Top-down interference and cortical responsiveness in face processing: a TMS-EEG study. Neuroimage 76, 24–32.

Mesulam, M., 1981. A cortical network for directed attention and unilateral neglect. Ann. Neurol.: Off. J. Am. Neurolog. Assoc. Child Neurol. Soc. 10 (4), 309–325.

Minarik, T., Berger, B., Althaus, L., Bader, V., Biebl, B., Brotzeller, F., Fusban, T., Hegemann, J., Jesteadt, L., Kalweit, L., Leitner, M., Linke, F., Nabielska, N., Reiter, T., Schmitt, D., Spraetz, A., & Sauseng, P. (2016). The importance of sample size for reproducibility of tDCS effects [data report]. Front. Hum. Neurosci., 10(453). doi:10.3389/fnhum.2016.00453.

Monte-Silva, K., Liebetanz, D., Grundey, J., Paulus, W., Nitsche, M.A., 2010. Dosage-dependent non-linear effect of L-dopa on human motor cortex plasticity. J. Physiol. 588 (18), 3415–3424. doi:10.1113/jphysiol.2010.190181.

Mosayebi Samani, M., Agboada, D., Jamil, A., Kuo, M.-F., Nitsche, M.A., 2019. Titrating the neuroplastic effects of cathodal transcranial direct current stimulation (tDCS) over the primary motor cortex. Cortex 119, 350–361.

Mosayebi-Samani, M., Agboada, D., Mutanen, T.P., Haueisen, J., Kuo, M.-F., Nitsche, M.A., 2023. Transferability of cathodal tDCS effects from the primary motor to the prefrontal cortex: a multimodal TMS-EEG study. Brain Stimul. 16 (2), 515–539.

Mutanen, T., Mäki, H., Ilmoniemi, R.J., 2013. The effect of stimulus parameters on TMS–EEG muscle artifacts. Brain Stimul. 6 (3), 371–376.

Nitsche, M.A., Paulus, W., 2000. Excitability changes induced in the human motor cortex by weak transcranial direct current stimulation. J. Physiol. (Lond.) 527 (Pt 3), 633.

Nitsche, M.A., Cohen, L.G., Wassermann, E.M., Priori, A., Lang, N., Antal, A., … Fregni, F., 2008. Transcranial direct current stimulation: state of the art 2008. Brain Stimul. 1 (3), 206–223.

Nobre, A.C., Gitelman, D.R., Dias, E.C., Mesulam, M.M., 2000. Covert visual spatial orienting and saccades: overlapping neural systems. Neuroimage 11 (3), 210–216.

Ohn, S.H., Park, C.-I., Yoo, W.-K., Ko, M.-H., Choi, K.P., Kim, G.-M., … Kim, Y.-H., 2008. Time-dependent effect of transcranial direct current stimulation on the enhancement of working memory. Neuroreport 19 (1), 43–47.

Oldfield, R.C., 1971. The assessment and analysis of handedness: the Edinburgh inventory. Neuropsychologia 9 (1), 97–113.

Oostenveld, R., Fries, P., Maris, E., Schoffelen, J.-M., 2011. FieldTrip: open source software for advanced analysis of MEG, EEG, and invasive electrophysiological data. Comput. Intell. Neurosci. *2011*.

Pantazis, D., Nichols, T.E., Baillet, S., Leahy, R.M., 2003. Spatiotemporal localization of significant activation in MEG using permutation tests. In: Biennial International Conference on Information Processing in Medical Imaging. Springer, pp. 512–523.

Pashler, H., 1988. Familiarity and visual change detection. Percept. Psychophys. 44 (4), 369–378.

Pellicciari, M.C., Brignani, D., Miniussi, C., 2013. Excitability modulation of the motor system induced by transcranial direct current stimulation: a multimodal approach. Neuroimage 83, 569–580.

Petersen, S.E., Robinson, D.L., Currie, J.N., 1989. Influences of lesions of parietal cortex on visual spatial attention in humans. Exp. Brain Res. 76 (2), 267–280.

Pisoni, A., Mattavelli, G., Papagno, C., Rosanova, M., Casali, A.G., Romero Lauro, L.J., 2018. Cognitive enhancement induced by anodal tDCS drives circuit-specific cortical plasticity. Cereb. Cortex 28 (4), 1132–1140.

Poreisz, C., Boros, K., Antal, A., Paulus, W., 2007. Safety aspects of transcranial direct current stimulation concerning healthy subjects and patients. Brain Res. Bull. 72 (4–6), 208–214.

Posner, M. I., 1980. Orienting of attention. Q. J. Exp. Psychol. 32 (1), 3–25.

Posner, M.I., Inhoff, A.W., Friedrich, F.J., Cohen, A., 1987. Isolating attentional systems: a cognitive-anatomical analysis. Psychobiology 15 (2), 107–121.

Posner, M. I., Nissen, M. J., Ogden, W. C., 2014. Attended and Unattended Processing Modes: The Role of Set for Spatial Location1. In: *Modes of perceiving and processing information*. Psychology Press, pp. 137–157.

Priori, A., Berardelli, A., Rona, S., Accornero, N., Manfredi, M., 1998. Polarization of the human motor cortex through the scalp. Neuroreport 9 (10), 2257–2260.

Purpura, D.P., McMurtry, J.G., 1965. Intracellular activities and evoked potential changes during polarization of motor cortex. J. Neurophysiol. 28 (1), 166–185.

R Core Team, 2022. R: A language and Environment For Statistical Computing Retrieved from.

Ridding, M.C., Ziemann, U., 2010. Determinants of the induction of cortical plasticity by non-invasive brain stimulation in healthy subjects. J. Physiol. (Lond.) 588 (13), 2291–2304.

Robison, M.K., McGuirk, W.P., Unsworth, N., 2017. No evidence for enhancements to visual working memory with transcranial direct current stimulation to prefrontal or posterior parietal cortices. Behav. Neurosci. 131 (4), 277.

Romero Lauro, L., Pisoni, A., Rosanova, M., Casarotto, S., Mattavelli, G., Bolognini, N., Vallar, G., et al., 2016. Localizing the Effects of Anodal tDCS At the Level of Cortical sources: a Reply to Bailey et al., 2015. In: Cortex, 74, pp. 323–328.

Romero Lauro, L., Rosanova, M., Mattavelli, G., Convento, S., Pisoni, A., Opitz, A., … Vallar, G., 2014. TDCS increases cortical excitability: direct evidence from TMS–EEG. Cortex 58, 99–111.

Rossi, S., Antal, A., Bestmann, S., Bikson, M., Brewer, C., Brockmöller, J., … Hallett, M., 2021. Safety and recommendations for TMS use in healthy subjects and patient populations, with updates on training, ethical and regulatory issues: Expert Guidelines. Clin. Neurophysiol. 132 (1), 269–306.

Rossi, S., Hallett, M., Rossini, P.M., Pascual-Leone, A., 2009. Safety, ethical considerations, and application guidelines for the use of transcranial magnetic stimulation in clinical practice and research. Clin. Neurophysiol. 120 (12), 2008–2039.

Roy, L.B., Sparing, R., Fink, G.R., Hesse, M.D., 2015. Modulation of attention functions by anodal tDCS on right PPC. Neuropsychologia 74, 96–107.

Sathappan, A.V., Luber, B.M., Lisanby, S.H., 2019. The dynamic duo: combining noninvasive brain stimulation with cognitive interventions. Prog. Neuropsychopharmacol. Biol. Psychiatry 89, 347–360.

Schroeder, P.A., Plewnia, C., 2017. Beneficial effects of cathodal transcranial direct current stimulation (tDCS) on cognitive performance. J. Cognit. Enhance. 1 (1), 5–9.

Siebner, H.R., Hartwigsen, G., Kassuba, T., Rothwell, J.C., 2009. How does transcranial magnetic stimulation modify neuronal activity in the brain? Implications for studies of cognition. Cortex 45 (9), 1035–1042.

Spooner, R.K., Wiesman, A.I., Proskovec, A.L., Heinrichs-Graham, E., Wilson, T.W., 2020. Prefrontal theta modulates sensorimotor gamma networks during the reorienting of attention. Hum. Brain Mapp. 41 (2), 520–529.

Stagg, C.J., Nitsche, M.A., 2011. Physiological basis of transcranial direct current stimulation. Neuroscientist 17 (1), 37–53.

Stagg, C.J., Antal, A., Nitsche, M.A., 2018. Physiology of transcranial direct current stimulation. J. ECT 34 (3), 144–152.

Tatti, E., Phillips, A.L., Paciorek, R., Romanella, S.M., Dettore, D., Di Lorenzo, G., … Santarnecchi, E., 2022. Boosting psychological change: combining non-invasive brain stimulation with psychotherapy. Neurosci. Biobehav. Rev., 104867.

Thakral, P.P., Slotnick, S.D., 2009. The role of parietal cortex during sustained visual spatial attention. Brain Res. 1302, 157–166.

Thiel, C.M., Zilles, K., Fink, G.R., 2004. Cerebral correlates of alerting, orienting and reorienting of visuospatial attention: an event-related fMRI study. Neuroimage 21 (1), 318–328.

Torriero, S., Mattavelli, G., Lo Gerfo, E., Romero Lauro, L., Actis-Grosso, R., Ricciardelli, P., 2019. FEF excitability in attentional bias: a TMS-EEG study. Front Behav. Neurosci. 12, 333.

Tseng, P., Hsu, T.-Y., Chang, C.-F., Tzeng, O.J.L., Hung, D.L., Muggleton, N.G., … Juan, C.-H., 2012. Unleashing potential: transcranial direct current stimulation over the right posterior parietal cortex improves change detection in low-performing individuals. J. Neurosci. 32 (31), 10554–10561.

Vallar, G., Perani, D., 1986. The anatomy of unilateral neglect after right-hemisphere stroke lesions. A clinical/CT-scan correlation study in man. Neuropsychologia 24 (5), 609–622.

Varoli, E., Pisoni, A., Mattavelli, G.C., Vergallito, A., Gallucci, A., Mauro, L.D., … Lauro, L.J.R., 2018. Tracking the effect of cathodal transcranial direct current stimulation on cortical excitability and connectivity by means of TMS-EEG. Front. Neurosci. 12 (MAY). doi:10.3389/fnins.2018.00319.

Veniero, D., Brignani, D., Thut, G., Miniussi, C., 2011. Alpha-generation as basic response-signature to transcranial magnetic stimulation (TMS) targeting the human resting motor cortex: a TMS/EEG co-registration study. Psychophysiology 48 (10), 1381–1389.

Vergallito, A., Feroldi, S., Pisoni, A., Romero Lauro, L.J., 2022. Inter-Individual variability in tDCS effects: a narrative review on the contribution of stable, variable, and contextual factors. Brain Sci. 12 (5), 522.

Vergallito, A., Gallucci, A., Pisoni, A., Punzi, M., Caselli, G., Ruggiero, G.M., … Lauro, L.J.R., 2021. Effectiveness of noninvasive brain stimulation in the treatment of anxiety disorders: a meta-analysis of sham or behaviour-controlled studies. J. Psychiatry Neurosci. 46 (6), E592–E614.

Vogel, E.K., Machizawa, M.G., 2004. Neural activity predicts individual differences in visual working memory capacity. Nature 428 (6984), 748–751.

Woods, A.J., Antal, A., Bikson, M., Boggio, P.S., Brunoni, A.R., Celnik, P., … Nitsche, M.A., 2016. A technical guide to tDCS, and related non-invasive brain stimulation tools. Clin. Neurophysiol. 127 (2), 1031–1048.